SINGS: The Spitzer Infrared Nearby Galaxies Survey
Fourth Data Delivery
May 2006

USER'S GUIDE

1. Introduction

This document describes the fourth data delivery of the Spitzer Legacy program SINGS. This delivery contains imaging data for all the galaxies in the sample and spectroscopic data for over 2/3 of the sample, plus examples of MIPS-SED data products. The document is organized as follows: section 2 lists the data products contained in this delivery and their general characteristics; sections 3, 4, 5, and 6 provide a description of the post-BCD processing for IRAC, MIPS, MIPS-SED, and IRS data, respectively; finally, section 7 briefly describes the data reduction steps of the ancillary data associated with this delivery.

For a complete description of the SINGS program, galaxy sample, and observing strategy, please refer to Kennicutt et al. 2003, PASP, 115, 928.

2. Content of the Data Delivery

2.1 Fourth-Delivery Sample and Data Products

The SINGS sample contains 75 galaxies, representative of a large range of properties of local normal galaxies (Kennicutt et al. 2003). Included in the present delivery are:

a. IRAC images of all 75 galaxies;
b. MIPS images of all 75 galaxies (except for the 70 μm and 160 μm images of NGC3034, see explanation in section 4.5);
c. IRS 2D maps and 1D spectra (in all four modules) for the nuclear regions of 65 galaxies; 3D spectral cubes for all modules for the nuclear regions of 48 galaxies; 2D maps and 1D spectral extractions for 50 extra-nuclear regions and 3D spectral cubes for 25 extra-nuclear regions in 9 galaxies;
d. MIPS-SED data cubes for 2 galaxies (Mrk33 and NGC3627) and a 1D extraction for 1 galaxy (Mrk33);
e. Optical images (B,V,R,I,Hα) for 73 galaxies (62 in Hα); galaxies missing any type of optical images are: NGC0855 and NGC4569; for NGC5055 and NGC5408 only Hα images are available;
f. Optical spectra for 66 galaxies. Galaxies missing optical spectroscopy are: HoII, NGC3034, NGC4236, NGC4631, DDO154, NGC5408, IC4710, NGC6822, NGC7552.

2.1.1 IRAC Mosaics

For each galaxy, 4 mosaics, one for each of the four IRAC bands, and the associated weight maps are delivered as single-extension FITS files. The pixel scale of the mosaics is 0.75 arcsec, and the flux units are MJy sr^{-1} (see, however, the Important Note About Photometric Calibration, section 3.7). The mosaics have standard orientation, with North up, East left.

Details of the post-BCD processing are given in Section 3.

2.1.2 MIPS Mosaics

For each galaxy, 3 mosaics, one for each of the MIPS bands, are delivered as single-extension FITS files. The pixel scale of the MIPS mosaics is wavelength-dependent: 1.5 arcsec at 24 μm, 4.5 arcsec at 70 μm, and 9.0 arcsec at 160 μm. The flux units are MJy sr^{-1}. The mosaics have orientation North up, East left.

Details on the post-BCD processing are given in section 4.

2.1.3 MIPS-SED Cubes

For two galaxies, MIPS-SED data cubes are delivered. The data products are single-extension FITS files. The data are in the form of spectral cubes, with the x- and y-axes representing the spatial dimension and the z-axis representing the spectral dimension. These data are calibrated in MJy/sr, and are background-subtracted. The pixel scale is matched to the 70 μm detector, 9.8 arcsec/pix, and the wavelength coverage is ~52-95 μm in 26 discrete steps. For one of the galaxies, mrk33, the spectrum has been extracted from the cube, and is delivered as a one-dimensional ASCII file (*.tbl).

The two datacubes, and the accompanying 1D extraction for one galaxy, are beta-products to provide examples of MIPS-SED products. The MIPS-SED AOTs were commissioned much later than other instrument/configuration AOTs (only about one year ago), hence the delayed data product delivery schedule.

Details on the post-BCD processing are given in section 5.

2.1.4 IRS Spectra, Maps, and Cubes

For 65 galaxies, six 2-dimensional maps of the nucleus (continuum-subtracted maps of [Ne III] 15.5 μm and [Si II] 34.8μm, complementary continuum maps at 15μm and 35μm, and maps of poly-cyclic aromatic hydrocarbon (PAH) emission at 7.6μm+8.6μm and 11.3μm) are being delivered. For each nuclear region, a single one-dimensional spectrum in all four IRS modules is also being delivered (Short-Low (SL) λ=5-15 μm, R=50-100; Long-Low (LL) λ=15-37μm, R=50-100; Short-High (SH) λ=10-20μm, R=600; and Long-High (LH) λ=20-37μm, R=600), ranging in size from 22.6″×14.8″ (high resolution, SH and LH) to 50″×33″ (low resolution, SL and LL). One-dimensional spectra are in ASCII (*.tbl), while the maps are in FITS format.

For 48 of the 65 galaxies, full three-dimensional spectral cubes in FITS format for all the modules are delivered. Maps and spectra are provided also for 50 extra-nuclear, optically selected regions in nine galaxies (HoII, NGC0628, NGC3031, NGC3521, NGC4736, NGC5194, NGC6822, NGC6946, and NGC7793). For these, three 2-dimensional maps (PAH emission at 7.7+8.6 μm, and 11.3 μm and a continuum map at 13.5 μm) and a corresponding one-dimensional spectrum in the SH, LH and SL modules are delivered. For 25 of the 50 extra-nuclear regions, 3D spectral cubes for all the modules are also delivered.

The units of the [NeIII] and [SiII] line maps are W m^{-2} sr^{-1}, while all other maps and spectra have units of MJy/sr.

Details on the data format and content, and on the post-BCD processing for the spectra are given in section 6.

2.1.5 Optical Images/Mosaics

Optical imaging data in the standard B, V, R, I broad-band filters and in narrow-band filters at the wavelength of the Hα+[NII] emission, plus continuum-subtracted Hα+[NII] images, are delivered for 69 of the 75 sample galaxies. Complete datasets (B,V,R,I,Hα) are available for only 61 galaxies, while for NGC5408 and NGC5055 only the continuum-subtracted Hα images are available (for NGC5408 also the associated continuum image is available).

The images are either single pointings, or mosaics of 2 or more adjacent and partially-overlapping frames. **T**he images are not background-subtracted.

All optical data are single extension FITS files (one file for each filter); they are flux calibrated and have astrometric solutions. Photometric and astrometric keywords are stored in the FITS headers.

The pixel scale is 0.305 arcsec (KPNO data) or 0.433 arcsec (CTIO data). The images have NE orientation, and are registered to a common frame. The flux scale is count/sec (CPS), and the relevant photometric keywords are: PHOTFLAM, to convert CPS to Jy, and ZPOINT, for the zeropoint.

More details on the optical images are given in section 7.1.

2.1.6 Optical One-dimensional Spectra

One-dimensional (1D) spectra in the wavelength range 0.36-0.70 μm are delivered for 66 of the 75 galaxies. For most galaxies, two spectra are delivered: the nuclear spectrum, and the central 20”x20” drift-scan spectrum.

The nuclear spectra are 2.5”x2.5” (KPNO) or 2.5”x3.0” (CTIO) aperture extractions of the brightest few central pixels. The 20”x20” drift-scan spectra target the central region of each galaxy, in a similar fashion to some of the IRS spectra. Both type of optical spectra are wavelength and flux calibrated. Resolution is ~8 Angstrom, and all fluxes are corrected for foreground Galactic extinction.

Nuclear and drift scan spectra are stored in separate ASCII files (*.txt). More details on the data and on individual galaxies are given in section 7.2.

2.2 File Name Convention

For each galaxy, multiple datasets are delivered, with the following filename convention:

- *IRAC mosaics*: ngcXXXX_v6.phot.#.fits (with #=1,2,3,4; e.g., ngc0337_v6.phot.1.fits)
- *MIPS mosaics*: ngcXXXX_mips#_crop_v4-0.fits (with #=24,70,160; e.g., ngc0337_mips24_crop_v4-0.fits)
- *MIPS-SED cubes*: ngcXXXX_mipssed_cube_v2-2.fits (ngc3627_mipssed_cube_v2-2.fits); for mrk33, a sample 1D extraction is provided, with name mrk33_DR4_SED.tbl
- *IRS Low-Res 1D spectra*: ngcXXXX_DR4_MD#_nuc_sp.tbl (MD=SL,LL; #=1,2, nuclear spectra) and ngcXXXX_extranuc_$$_DR4_MD#_sp.tbl (extra-nuclear spectra, $$=number of extranuclear region)
- *IRS Low-Res 1D Estimated Background Spectra (selected sources only):* ngcXXXX_DR4_SL#sky_sp.tbl (#=1,2)
- *IRS High-Res 1D spectra*: ngcXXXX_DR4_MD_nuc_sp.tbl (MD=SH,LH, nuclear spectra) and ngcXXXX_ extranuc_$$_DR4_MD_sp.tbl (extranuclear spectra, $$=number of the extranuclear region)
- *IRS 2D Maps*: ngcXXXX_DR4_MD#_line.fits and ngcXXXX_extranuc_$$_DR4_MD#_line.fits (line=neIII, siII, pah_8, pah_11_3, extranuc=extranuclear region), ngcXXXX_DR4_MD#_line_cont.fits (line=neIII, siII) and ngcXXX_extranuc_$$_DR4_MD#_cont_13.fits
- *IRS 3D Cubes*: ngcXXXX_DR4_MD#_cube.fits and ngcXXXX_DR4_MD#_cube_unc.fits (cube and cube's uncertainty, respectively); for the extranuclear regions: ngcXXXX_extranuc_$$_DR4_MD#_cube.fits and ngcXXXX_extranuc_$$_DR4_MD#_cube_unc.fits ($$=number of extranuclear region)
- *Optical images/mosaics*: ngcXXXX_#_dr4.fits (with #=B,V,R,I,HA,HA_SUB, e.g., ngc5194_HA_dr4.fits)
- *Optical 1D spectra*: ngcXXXX_nuclear_002_5.txt, and ngcXXXX_drift_020_020.txt.

3. IRAC Data Products and Post-BCD Processing

IMPORTANT NOTE FOR DR4:

IRAC DR4 data products have a slightly degraded quality relative to similar DR3 products, for the following reason. The BCDs used in this data release are from the S13 version of the SSC IRAC pipeline. In this pipeline, the step that removes jailbars from IRAC frames has been switched off. As a result, all BCDs have jailbars in them. The SSC has released an IDL software to mitigate the jailbars in the BCDs. The software is only partially effective, and as a result many of the SINGS IRAC mosaics show residual jailbar structure in the background.

Preliminary measurements suggest that the impact of the jailbar residual on photometry is small. Point sources with peak fluxes down to 0.3 MJy/sr have their photometry affected by 3% or less.

The expectation is that the S14 BCDs will have this problem corrected, and future SINGS mosaics will not show it.

IRAC DR4 mosaics offer, however, the following advantages over the DR3 version:

a. Better astrometry, both between bands and with MIPS mosaics;
b. More centrally concentrated PSFs (better registrations between mosaic tiles);
c. Background removed from all mosaics.

3.1 Introduction

The SINGS IRAC images are created from multiple Spitzer images in either a mosaic or single field dither pattern. The fundamental data used for these are the Version 13 Basic Calibrated Data (BCD) images produced by the Spitzer Science Center (SSC). These data have already undergone a number of processing steps including conversion from engineering to scientific units, flat fielding and bias subtraction. The SINGS IRAC pipeline further processes these data to deal with a number of issues including frame geometric distortion and rotation, residual flat fielding, cosmic rays, frame alignment, and bias drift. Frames are finally combined using the drizzle algorithm to maximize resolution from the individual sub-sampled images. The major observation and processing steps are detailed below.

3.2 Data Products

The IRAC data products contained in this delivery are single-extension FITS files, two files for each IRAC band for each galaxy: the first FITS file is the science mosaic (*.1.fits, .2.fits, etc.) and the second FITS file is the weight map (*.1_wt.fits, *.2_wt.fits, etc.). The science images are calibrated in MJy sr^{-1}, and have pixel size of 0.75 arcsec. The weight maps contain the information on the number of frames that were used to create the science mosaics at each pixel (value= # frames x10); the pixel size of the weight maps is the same as the science mosaics.

The original header keywords are retained, plus others added as a result of the post-BCD processing. In particular, astrometry is stored using FITS standard WCS coordinate keywords; the flux scale is stored in the BUNIT keyword; and the background subtraction and its value are stored in the keywords BACK_SUB (performed=T, not performed=F) and BACKGRND (value), respectively.

A note about background subtraction: only constant level backgrounds have been subtracted from the images. Spatially variable backgrounds (see, e.g., NGC6946) have not been removed.

3.3 Observational Strategy

Observations were carried out in accordance with the SINGS IRAC observing strategy (Kennicutt et al. 2003). For galaxies larger than the 5' size of the IRAC detectors, observations are taken in a mosaic pattern, offsetting the field of view by ~50% each time. This process is repeated twice, with observations separated by at least 24 hours to best correct for asteroids and detector artifacts. Points in the central mosaic regions are thus imaged eight times and the outermost regions four times. Galaxies fitting in a single IRAC field are imaged using two sets of four dithered observations, again resulting in points being observed eight times over the bulk of the final images. Observations are 30 seconds in duration with an additional one second exposure taken at each pointing to provide data in cases where the main observation is saturated.

3.4 Image Processing

The steps performed by the SINGS IRAC pipeline are the following:

a. Geometric Distortion and Image Rotation

BCD images contain geometric distortions caused by IRAC's off-axis location in the Spitzer focal plane. The magnitude of these distortions is up to 2.2". These are corrected for in the SINGS IRAC pipeline using the most recent coefficient tables supplied by the GOODS team. Frames (single-exposure images) from the second set of exposures are also rotated to the orientation of the first using the header position angle difference between the first images of each observation set.

b. Bias Structure

At present there is some residual bias structure in the IRAC BCD data, particularly affecting band 3. To address this issue, IRAC band 3 frames for galaxies observed with a mosaic pattern are median combined and the result subtracted from each frame. This method is not applied to observations obtained with a dither pattern (small galaxies), as in this case the object occupies a large fraction of each frame, thus strongly affecting the median.

c. Image Offsets

Offsets between individual BCD images are determined through image cross-correlation. In this process, rough cosmic ray rejection is first carried out by comparing

the short and long IRAC exposures at each pointing. Any two frames with at least 10,000 pixels in common are cross-correlated with each other. Individual frame pair cross-correlation results from all four bands are combined for maximal accuracy, weighting offsets by their errors and applying outlier rejection. Within each band, a consistent solution for frame positions is then obtained through least square fitting. Accuracy for this process varies from galaxy to galaxy, but is generally in the range 0.1 pixels. Extra positional offsets have been added for large (mosaiced) galaxies with separate fields of view, improving the final astrometric solutions for these galaxies.

d. Bias Drift

IRAC images are at present still subject to full frame DC bias drift with time. To correct for this, the SINGS IRAC pipeline matches the bottom 20-th percentile flux level in regions of overlap (to prevent contamination from Muxbleed effects) and determines any DC offset between overlapping frames. This offset is assumed to be due to the bias drift. χ^2 minimization is again applied to find a consistent solution for all frames and the appropriate DC offsets applied.
The DC-offset matching routine has been improved for galaxies with separate fields of view or fields of view with minimal overlap. An extra background offset was added between BCDs in separate views of field before the χ^2 minimization is carried out.

e. Cosmic Rays
Final cosmic ray masks are created using standard drizzle methods (see the HST Dither Handbook: http://www.stsci.edu/instruments/wfpc2/Wfpc2_driz/dither_handbook.html). For DR4, The SINGS IRAC pipeline switched from Drizzle (used up to and including DR3) to Wdrizzle. both tasks within the IRAF/STSDAS package.

Each image is first drizzled to correct for geometric distortion. The weight files from this step are also used to create pixel masks. Following this, the images are median combined to reject cosmic rays. These images are then 'blotted' - a step that effectively reverses the steps so far - to create images equivalent to the original input images but without cosmic rays. Finally, a spatial derivative is calculated to assess the effects of blurring in the median image (Dither Handbook, page 60) and the original and blotted images are compared to obtain a cosmic ray mask for each image.

f. Background Subtraction

Background levels are determined by fitting a constant across each mosaic's regions free of the target. This is accomplished by plotting an histogram of the pixel levels in a region outside of the galaxy and fitting a Gaussian through the pixels' distribution. The peak of the Gaussian is adopted as background level for the mosaic. The constant value subtracted from the mosaic is stored in the keyword BACKGRND.

The user is cautioned that in some cases, a constant background level is only an approximation of the actual background, as variations across the mosaic's field has been noted in some cases.

g. Final Images

The final step in the SINGS IRAC pipeline is to drizzle the original long exposures together, applying the geometric distortion and rotation corrections, cosmic ray masks and determined image offsets. In this process, the output pixels are scaled to 0.75 arcsec. The routine Wdrizzle is used for the final step, which also allows us to fix the reference pixel of the final mosaic (now selected to be at the center of the galaxy). The drop factor is set to 0.75, which is chosen to yield fully sampled images with maximal resolution. A correction factor is also applied to the final images to maintain accurate photometry given the change in pixel size. Blank pixels in the final mosaic images are set to IEEE NaN (not a number).

The final drizzle step combines together the images from the two different AORs, thus removing asteroids in the process.

Final images are delivered in north up orientation using the quoted position angle, which is now set to zero.

3.5 Known Problems and Image Artifacts

A few of band 3 and 4 images show a persistent gradient in the background, which results in changes by (typically) up to 0.1 MJy/sr in the level between one side of the image and the other.

Finally, users are cautioned to be aware of standard IRAC detector artifacts that may also be present in the SINGS data, although our observing and mosaicing strategies are designed to attempt to minimize these artifacts. These are detailed extensively elsewhere (Hora et al. 2004, SPIE, in press; Fazio et al. 2004, ApJS 154, 10) and include: persistent images in channels 1 and 4, diffuse stray light, stray light from point sources, Muxbleed, column pulldown and banding, remaining full-frame bias and ghost images. Because we combine two epochs of observations that are slightly rotated and we match the backgrounds between overlapping BCD images, some of the detector anomalies are mitigated in our final mosaics.

3.6 Important Note on Photometric Calibration

The units of the SINGS IRAC mosaics are the same as the original BCDs delivered by the SSC. No aperture corrections have been applied to the final data products. The user should be cautioned that when performing aperture photometry, aperture corrections need to be applied even for relatively large apertures, and that the calibration for point sources is different from that of extended sources (Jarrett 2006, Spitzer Science Center Publications, http://spider.ipac.caltech.edu/staff/jarrett/irac/calibration/).

IRAC calibrations are performed using a 12” radius aperture on stars, and the units of MJy/sr of the mosaics refer to this specific aperture. Aperture correction factors are given in the Infrared Array Data Handbook, Version 2.0, section 5.5.

3.7 Notes on Individual Galaxies

NGC3034: No background subtraction applied to this galaxy's mosaics. For the BCDs pointing at the galaxy's center, extensive masking was applied to remove detector's artifacts.

NGC3198: The channel 3 image of this galaxy shows a `saddle-shaped' background, with a negative variation of 0.1 MJy/sr at the center relative to the edges.

NGC 5408: Mosaics contain some very bright foreground stars. The centers of some of these have been rejected in the Band 1 image by the cosmic ray flagging routine.

4. MIPS – Imaging Data Products and Post-BCD Processing

4.1 Introduction

The SINGS MIPS mosaics were created from multiple Spitzer images obtained in scan-mapping mode, and fully processed with the MIPS Data Analysis Tool (MIPS DAT, Gordon et al. 2005, PASP, 117, 503). The major observation and processing steps are detailed below. This delivery contains MIPS images for all 75 SINGS galaxies, except for the 70 μm and 160 μm images of NGC3034. These two images will be delivered at a later date, since they require special processing and handling(due to the brightness of the source).

4.2 Data Products

The SINGS MIPS data products are single-extension FITS files, one file for each MIPS band (*_mips24_crop_v4-0.fits, *_mips70_crop_v4-0.fits, and *_mips160_crop_v4-0.fits). The images are calibrated in MJy sr^{-1}, and have pixel size 1.5, 4.5 and 9.0 arcsec for the 24 μm, 70 μm, and 160 μm mosaics, respectively. The pixel sizes of the MIPS mosaics have been chosen to adequately sample the point spread function and at the same time be an approximate integer multiple of the IRAC mosaics' pixel scale (approximately 0.75 arcsec, see section 3). Constant backgrounds have been subtracted from the data as part of the data processing. Spatially variable backgrounds, such as cirrus structure, have not been removed.

All original fits header information has been retained. The headers' content has been re-arranged so that basic information on the observations, the target, and coordinates, and the pixel sizes appears first in the listing. Among the relevant keywords: the mosaics' astrometry is stored in the standard FITS WCS keywords; the flux units are stored in ZUNITS; and, as for the IRAC images, the background subtraction and its value are stored in the keywords BACK_SUB (performed=T, not performed=F) and BACKGRND (value), respectively. All other information, which includes details on the observations and the data processing, is located after these basic keywords.

4.3 Observational Strategy

The MIPS observations were obtained using the scan-mapping mode in two separate visits to the galaxy. Separate visits allow asteroids to be recognized and provide observations at orientations up to a few degrees apart to ease removal of detector artifacts. As a result of redundancy inherent in the scan-mapping mode, each pixel in the core map area was effectively observed 40, 20, and 4 times at 24, 70, and 160 microns, respectively, resulting in integration times per pixel of 160 s, 80 s, and 16 s, respectively.

4.4 Post-BCD Image Processing

The MIPS data were processed using the MIPS DAT versions 3.06 along with additional customized processing software. The processing steps are as follows.

1. For the 70 and 160 μm data, a linear fit is applied to the ramps (the counts accumulated in each pixel during the non-destructive readouts), and slopes are derived. This step also removes cosmic rays and readout jumps and applies an electronic nonlinearity correction.

2. The initial processing of the 24 μm data is different from the 70 and 160 μm data, as slopes are already fit to the 24 μm data on the spacecraft. Thus, the 24 μm images are processed through a droop correction (that removes an excess signal in each pixel that is proportional to the signal in the entire array), correction for non-linearity in the ramps, and dark current subtraction.

3. Telescope optical signatures and time-dependent responsivity variations in the detector elements are removed from the data, in the following way:

   a. For the 24 μm images, flatfielding is performed in two steps. First, scan mirror position dependent flatfields are applied to the data (to correct dark spots caused by particulate matter on the scan mirror that shift in position from frame to frame). These flatfields are created from a superflat with a superimposed spot map that is shifted to match the spots in the individual scan legs. Next, scan mirror position independent flats are created from off-target data in the data from each AOR; these flatfields are applied to the data to remove any residuals left by the scan-mirror-dependent flats. Additionally, a readout offset correction is applied between the flatfielding steps to correct variations across the columns in the images. Latent images in the 24 μm data (from bright sources and bright cosmic ray hits) are masked out after the flatfielding. Any frames with severe problems (such as severe "jailbar" pattern effects or deviations in the median values above the 10% level) are also masked out (unless they include the target). Following this, the background is subtracted from the individual frames of data. This is done by finding the background levels as a function of time for each individual scan leg while excluding the target and other bright sources, then fitting a third order polynomial to the background values. The function is then used to calculate the background for each frame, and this background is subtracted.

   b. The stimflash frames taken by the telescope are used for responsivity corrections of the 70 and 160 μm arrays. Next, the dark current is subtracted, and illumination corrections are applied to the data. Following this, short-term variations in the images caused by drift are subtracted. This last step also subtracts the background from the data.

4. A preliminary mosaic is made with the resolution set to the native pixel resolution of the MIPS detectors. During this mosaicking process, the individual frames of data are rewritten. A statistical analysis is performed on all pixels that overlap, and pixels that deviate at the 3σ level are masked out in the rewritten frames. This step effectively filters out cosmic rays and other transient phenomena.

5. The individual data frames are visually and statistically inspected for erroneously high or low pixel values and bad frames. Any such data that are found are set to NaN for further data processing.

6. Final mosaics are made from the individual frames. Data from both AORs are mosaicked together. After this step, backgrounds are subtracted from the data in all wavebands using the following methods:

   a. Constant-level backgrounds in the 24 μm data are measured in multiple small circular regions specifically chosen by eye near the optical disk to avoid bright background or foreground sources.

   b. Constant-level backgrounds in the 70 and 160 micron images are measured in two or more regions that straddle the target. These regions cover an area at least twice as large as the galaxy. They are chosen by eye so as to match the background region under the target itself and to avoid bright sources. These background values are then subtracted from the final map. Since the short-term drift removal does subtract most of the background, this step removes only a residual offset.

7. After the mosaics are created, the images are multiplied by a final calibration factor that converts the MIPS units into MJy sr^{-1}. The factors are the following (keyword JANSCALE in the image headers):

   24 μm: 0.0447 MJy sr^{-1} $MIPS\_units^{-1}$

   70 μm: 702 MJy sr^{-1} $MIPS\_units^{-1}$

   160 μm: 44.7 MJy sr^{-1} $MIPS\_units^{-1}$

   The mosaics in this delivery have been cropped to sizes that include all of the galaxies' optical disks and any nearby galaxy or extended structure. The cropped images also include a minimum of 40" space between the edge of the optical disk and the edge of the image, so that sufficient information for measuring the background is provided.

4.5 Special Cases, Known Problems and Uncertainties

Special processing for NGC 7331 70 μm data

The NGC 7331 70 μm data were taken before the bias voltages of the MIPS 70 μm detector were adjusted to their current values. As a result, the raw data contain significant latent images from the stimflash that need to be removed to process the data. Because of this, the NGC 7331 70 μm data were not processed through the software that removes the short term drift variations. The quality of the data is also worse than the quality of the other 70μm data in this delivery.

Special processing for NGC 3034 24 μm data

Due to the brightness of the target, special procedures were required to reduce the NGC 3034 data. The saturating nucleus introduced artifacts on the array, so separate mosaics were produced using just those DCEs which contained the nucleus (the "inner" mosaic), and all other DCEs (the "outer" mosaic), aligned in array coordinates to facilitate further artifact removal. The inner mosaic was processed further to improve the droop correction and to subtract a bar-shaped artifact which ran through the saturated nucleus perpendicular to the scan direction (i.e., along the short axis of the map). A small offset (~10 counts) was added to the inner mosaic to match the DC level of the outer mosaic. The two maps were then combined, using data from the inner mosaic to fill in the hole in the outer mosaic. The combined map, ngc3034_24_image_v4-0.fits, was then rotated to the standard N up, E left orientation using the IDL Astronomy Library's "hastrom" task.

The 70 μm and 160 μm data of NGC3034

The 70 μm and 160 μm images of NGC3034 require special handling and processing, because of the strong non-linearity present in the data. Reduction efforts are still on-going. Mosaics in these bands for this galaxy will be delivered in the future.

Streaking in the 70 μm data

Bright sources in the 70 μm data produce negative latent images that are manifested as negative streaks in the data. Sometimes positive streaks on the opposite side of the bright sources from the negative streaks are also apparent. These positive streaks are regions where, partly because of the negative latent images, the background is undersubtracted. Work is underway to correct the negative streaking, which should also lead to a reduction of the positive streaking.

In the current delivery, the following galaxies have the most severely 'streak-affected' 70 μm images: NGC 1097, NGC 1266, NGC 1316, NGC 1377, NGC 1482, NGC 1510, NGC 1566, NGC 2798, NGC 3031, NGC 3049, NGC 3190, NGC 3265, NGC 3351, NGC 3521, NGC 3621, NGC 3627, NGC 4254, NGC 4321, NGC 4450, NGC 4536, NGC 4569, NGC 4579, NGC 4625, NGC 4631, NGC 4736, NGC 4826, NGC 5033, NGC 5055, NGC 5408, NGC 5713, NGC 6946, NGC 7552

Non-linearity Effects in the 70 μm data

The MIPS 70 μm array is affected by nonlinearity at high count rates. This effect becomes significant in point sources at 3 Jy, where measured counts are ~10% too low, and the effect becomes larger for brighter sources (Gordon et al., in preparation). Since the effect is to depress counts on the brightest pixels, it can be alleviated in unresolved sources by performing photometry via PSF fitting, which delays the onset until ~10 Jy.

However, PSF fitting is generally not applicable to extended targets like the SINGS galaxies. In the case of compact sources, the 70 μm nonlinearity decreases the global fluxes of any source brighter than about 3 Jy. For example, the global flux of the most compact galaxy in the SINGS sample, Mrk 33, is reduced by ~15% by this effect. Furthermore, it is likely that the nonlinearity acts to depress the response of any pixel viewing a high flux density, so the user is cautioned that the 70 μm profiles of galaxies with high central surface brightnesses (above ~200 MJy/sr) may have been flattened somewhat by this effect. However, global fluxes of extended sources, with significant contributions from low-surface brightness regions, are not affected significantly.

SINGS targets likely to be impacted by the 70 μm non--linearity include: Mrk 33, NGC 1097, NGC 1266, NGC 1377, NGC 1482, NGC 2798, NGC 3351, NGC 3627, NGC 4536, NGC 5195, and NGC 7552.

A correction for the nonlinearity is under development, but has not yet been implemented at this time of this writing. The plan is to deliver MIPS mosaics corrected for this effect in DR5.

Artifacts near Bright Sources in the 24 μm data

In some cases, bright sources in the 24 μm data trigger a strong "jailbar" effect and a droop effect visible as a step function in the background. Work is underway to properly correct both of these effects.

In the current delivery, the only galaxies strongly affected by this problem (on target) are NGC 1482, NGC 2798, NGC 3034, NGC 6946, and NGC 7552. Also note the special processing for NGC 3034 above.

Photometric Uncertainties

Currently the estimated calibration uncertainties for MIPS extended object photometry are 4%, 7%, and 12% for the 24, 70, and 160 μm data, respectively. The uncertainty figure for the 70 μm images refers only to sources unaffected by the non—linearity discussed above.

5. MIPS-SED Data Products and Post-BCD Processing

In DR4, two MIPS-SED datacubes and one 1D extraction from one of the cubes are delivered as beta-products. This is the first delivery of such products performed by SINGS.

The MIPS-SED AOTs were commissioned much later than other instrument/configuration AOTs (only about one year ago), which accounts for the delayed data product delivery schedule.

More/improved data products will be delivered starting with DR5.

5.1 Data Products

The SINGS MIPS SED data products are single-extension FITS files. The naming convention is *_mipssed_cube_v2-2.fits. The data are in the form of spectral cubes, with the x- and y-axes representing the spatial dimension and the z-axis representing the spectral dimension. These data are calibrated in MJy/sr, and the backgrounds have been subtracted from the data (as described in section 5.3).

The x- and y- dimensions of the individual pixels are set to match the dimensions of an individual 70 micron pixel (9".8). The data also have the same orientation as the observations.

The keywords in the fits headers provide both the WCS information for the position of the pixels and the spectral information for determining the correspondence between the z-axis and wavelength. This relation is given by:

$$\lambda\ (\mu m) = 1.71*(z-16)+77.91$$

The wavelength coverage of the spectral cubes is 52.26—95.01 μm, in 26 steps (frames in the data cube).
A new header is created for the MIPS SED data products, but the original fits header information from the central row of the map is attached to the bottom of the new header. The arrangement of the header information is similar to that for the MIPS image data products.

5.2 Observing Strategy

The SINGS MIPS SED data are obtained in mapping mode, in a grid of 7 positions offset by half the slit width. The resulting map is about 1' wide and 3' to 6' (depending on the size of the galaxy) long. At each map position, 2-3 cycles of the SED AOT (which consists of on-source observations alternated with background observations 3' away) are executed, using 10-second exposures. The total exposure depth (except for a 1-pixel border) is thus 240-360 seconds per point.

5.3 Post-BCD SED Processing

The MIPS SED data were processed using the MIPS DAT version 3.06 along with additional customized processing software. The processing steps are as follows.

1. The first data processing steps are identical to Steps 1 and 3b (minus the drift subtraction) described for the 70 μm image processing in section 4.4.
2. For each on-target frame, we make a background frame by median combining the two off-target frames taken immediately before the on-target frame and the two off-target frames taken immediately after the on-target frame. Note that we only use three off-target frames to build the background frame if one off-target frame was taken before or after the on-target observations. We then subtract this background frame from the on-target frame.
3. Mosaics are made of each slit position. This produces multiple on-target frames with the x-axis representing the spatial dimension and the y-axis representing the spectral dimension.
4. The first three columns of each row are blanked out. These columns correspond to noisy columns in some of the calibration images.
5. The data are calibrated to MJy/sr using flux conversion factors derived from MIPS SED observations of Arcturus.
6. A spectral cube, with the x- and y-axes representing the spatial dimension and the z-axis representing the spectral dimension, is built from the individual rows. In locations in the spectral cube where two or more frames overlap, the average of the values from all overlapping frames is used.

Note that only rows 1-26 are used to construct these spectral cubes. A second-order spectrum is visible starting with row 27, so rows 27-32 are not used for the final cube.

5.4 Example: One-dimensional Extraction of the Mrk33 MIPS-SED Spectrum

For the purpose of comparing dust emission models to data, the slope of the one-dimensional (1D) spectrum is a key piece of information that can be extracted from the SINGS data cube built from MIPS SED measurements. Aperture corrections are critical to an accurate measurement of the slope of this spectrum, but can be difficult to compute for the galaxies observed by SINGS, most of which are resolved into complex structures at the MIPS SED wavelengths (52 - 95 μm). For a point source, however, the corrections are straightforward to compute, so we provide a sample extraction for the SINGS galaxy Mrk 33, which is nearly unresolved by MIPS at these wavelengths.

5.4.1 Data Format

The 1D spectrum of Mrk33 is provided as an ASCII file (*.tbl). The file consists of a header followed by the data in two columns: wavelength (in μm) and flux intensity (in MJy/sr).

5.4.2 Extraction Procedure

From each plane along axis 3 (spectral axis) of the Mrk 33 data cube, the flux of Mrk 33 was measured using an aperture 3 pixels (the pixel size is 9.8") in radius. The aperture correction is based on model point spread functions computed using STinyTim in 10 μm increments from 50 to 100 μm. To simulate the effects of the MIPS sampling of the data, the models were convolved with a square kernel 1.7 native (i.e., 9.8") pixels in width, which was found empirically to match the profile of an unresolved source. An aperture identical to that used on the Mrk 33 data was used to measure counts from the smoothed models, and a function was fit to the derived aperture corrections:

$$\text{aperture correction} = 0.664 + 0.0096 * \lambda\,(\mu\text{m})$$

The Mrk 33 aperture measurements were multiplied by this function, which has a significant effect on the slope of the final spectrum: the aperture correction rises by nearly 40% from 1.163 at 52 μm to 1.576 at 95 μm.

The resulting continuum slope for Mrk 33 rises by ~0.02 Jy/μm, consistent with the slope derived from the color-corrected IRAS/PSC fluxes of 4.52 Jy at 60 μm and 5.32 Jy at 100 μm. The continuum level at the nominal wavelength of the MIPS 70 μm band, 71.42 μm, is 4.8 Jy, consistent with the 4.9 Jy derived from the SINGS 70 μm image of this galaxy after color correction and a 10% correction for nonlinearity on this bright source.

6. IRS Data Products and Post-BCD Processing

6.1 Observations and Data Products

All SINGS IRS observations are taken in the Spectral Mapping Mode, in which the slit is moved in a raster pattern to build up a redundantly sampled spectral map of the target region. In this fourth data release we provide an extensive set of spectral data products. For all 65 SINGS galaxies where we have IRS data, we deliver six 2-dimensional maps of the nuclear region (maps of poly-cyclic aromatic hydrocarbon emission at 7.6μm+8.6μm and 11.3μm, continuum-subtracted maps of [Ne III] and [Si II], and complementary continuum maps at 15μm and 35μm). One-dimensional spectra for each nuclear region in all four IRS modules are also delivered (Short-Low (SL) λ=5-15 μm; Long-Low (LL) λ=15-37μm; Short-High (SH) λ=10-20μm; and Long-High (LH) λ=20-37μm), ranging in size from 22.6″×14.8″ (high resolution, SH and LH) to 50″×33″ (low resolution, SL and LL). An example illustrating these extraction regions overlaid on the 8μm image of M51 is shown in Fig. 1.

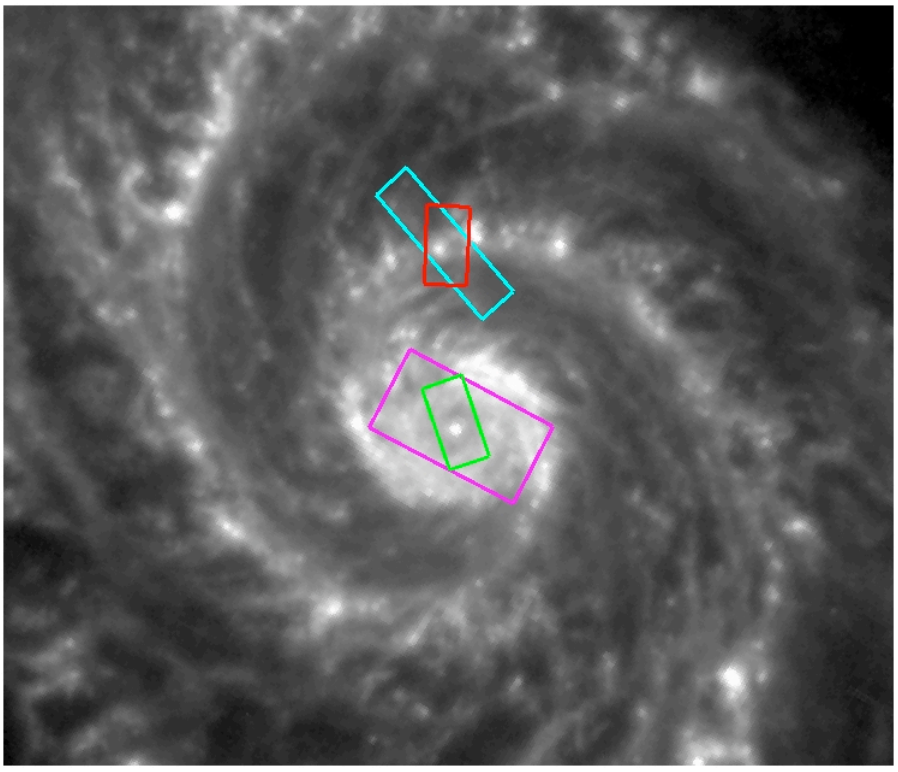

Figure 1: The 8μm image of M51, with example extraction regions for the IRS spectra in this delivery, shown with the following overlays: magenta: low resolution nuclear spectra, green: high resolution nuclear spectra, red: high resolution extra-nuclear region 00, and cyan: low resolution extra-nuclear region 00. In this particular case, the region mapped around the extra-nuclear region is not perfectly centered on the 8μm peak because the region was optically selected and the peak of emission is offset from the mid-

infrared emission.

For 48 of 65 galaxies, a full three-dimensional spectral cube in FITS format for all the modules and orders is provided (see Table 2). For 50 extra-nuclear regions from nine galaxies (HoII, NGC0628, NGC3031, NGC3521, NGC4736, NGC5194, NGC6822, NGC6946, and NGC7793, see Table 3), three 2-dimensional maps (PAH emission at 7.7+8.6 μm, and 11.3 μm and a continuum map from 13.06--13.43 μm) and a corresponding one-dimensional spectrum in the SH, LH and SL modules are delivered. Full three-dimensional cubes for 25 extra-nuclear regions are also provided with this delivery. An example of one such extra-nuclear region is shown in Figure 1.

6.2 File Format and Naming Convention

All spectra are formatted as ASCII files in the IPAC table format. The headers give the date of each observation, corresponding to the first data collection event in the spectral map, as well as the location of the regions over which the data were extracted. Compared to the previous delivery, there are two important enhancements: a) An estimate of the uncertainties is provided with both the one-dimensional spectra and the cubes, and b) In addition to an aperture loss correction, a theoretical slit loss correction factor has been calculated and applied to the data (see details in §6.3).

Low-Resolution Spectra are divided by module and order, with the naming convention:

ngcXXXX_DR4_MD#_nuc_sp.tbl (nuclear spectra)
ngcXXXX_extranuc_$$_DR4_MD#_sp.tbl (extra-nuclear spectra)

where "MD" is the module (SL, LL), "#" is the order (1 or 2), and $$ is the number of the extra-nuclear region ordered according to the observations date. Each file consists of a header followed by the data in three columns: wavelength (in μm), and flux intensity (in MJy/sr), and uncertainty in flux intensity (MJy/sr).

For those sources listed as "Model 1D" in the second column of Table 2 and 3, estimated background spectra for SL1 and SL2 are provided, with names

ngcXXXX_DR4_SL#sky_sp.tbl.

High-Resolution spectra are also divided by module, with the naming convention

ngcXXXX_ DR4_MD_nuc_sp.tbl (nuclear spectra)
ngcXXXX_ extranuc_$$_DR4_MD_sp.tbl (extra-nuclear spectra)

where "MD" is the module, either "SH" or "LH", and $$ is the number of the extra-nuclear region. Each file consists of a header followed by the data in three columns: wavelength (in μm), and flux intensity (in MJy/sr), and the uncertainty in the flux intensity (MJy/sr). Data from overlapping orders are interpolated and averaged in each high-resolution spectrum.

All maps are formatted as FITS files with header information describing the wavelength range of the continuum region used to construct the map. The maps are labeled

ngcXXXX_DR4_MD#_{neIII,siII,pah_8,pah_11_3}.fits
ngcXXXX_extranuc_$$_DR4_MD#_{neIII,siII,pah_8,pah_11_3}.fits

where neIII, siII are the continuum subtracted neon and silicon line maps, the pah_8 and pah_11_3 are the 7.6μm+8.6μm and 11.3μm maps respectively. The associated continuum maps are labeled

ngcXXXX_DR4_MD#_{neIII,siII}_cont.fits

The continuum map for the extranuclear regions is labeled:

ngcXXXX_extranuc_$$_DR4_MD#_cont_13.fits

Note that the units of [NeIII] and [SiII] line maps are W m^{-2} sr^{-1}, while all other maps and spectra have units MJy/sr. Examples of some of these products are shown in Figure 2.

The spectral cubes and uncertainty cubes are in standard 3D FITS Format, with the coordinates of the spectral dimension specified in a look-up table following the new spectral FITS standard of Greisen et al. (2005). Since this standard is new, most existing tools do not yet handle spectral coordinate axes properly. The vector specifying wavelengths for each plane of the spectral cube can be retrieved from the binary table in the first and only FITS extension.

The cubes are labeled as follows:

ngcXXXX_DR4_MD#_cube.fits (nuclear regions)
ngcXXXX_DR4_MD#_cube_unc.fits (uncertainty cube for nuclear regions)
ngcXXXX_extranuc_$$_DR4_MD#_cube.fits (extra-nuclear regions)
ngcXXXX_extranuc_$$_DR4_MD#_cube_unc.fits (uncert for extra-nuc regions)

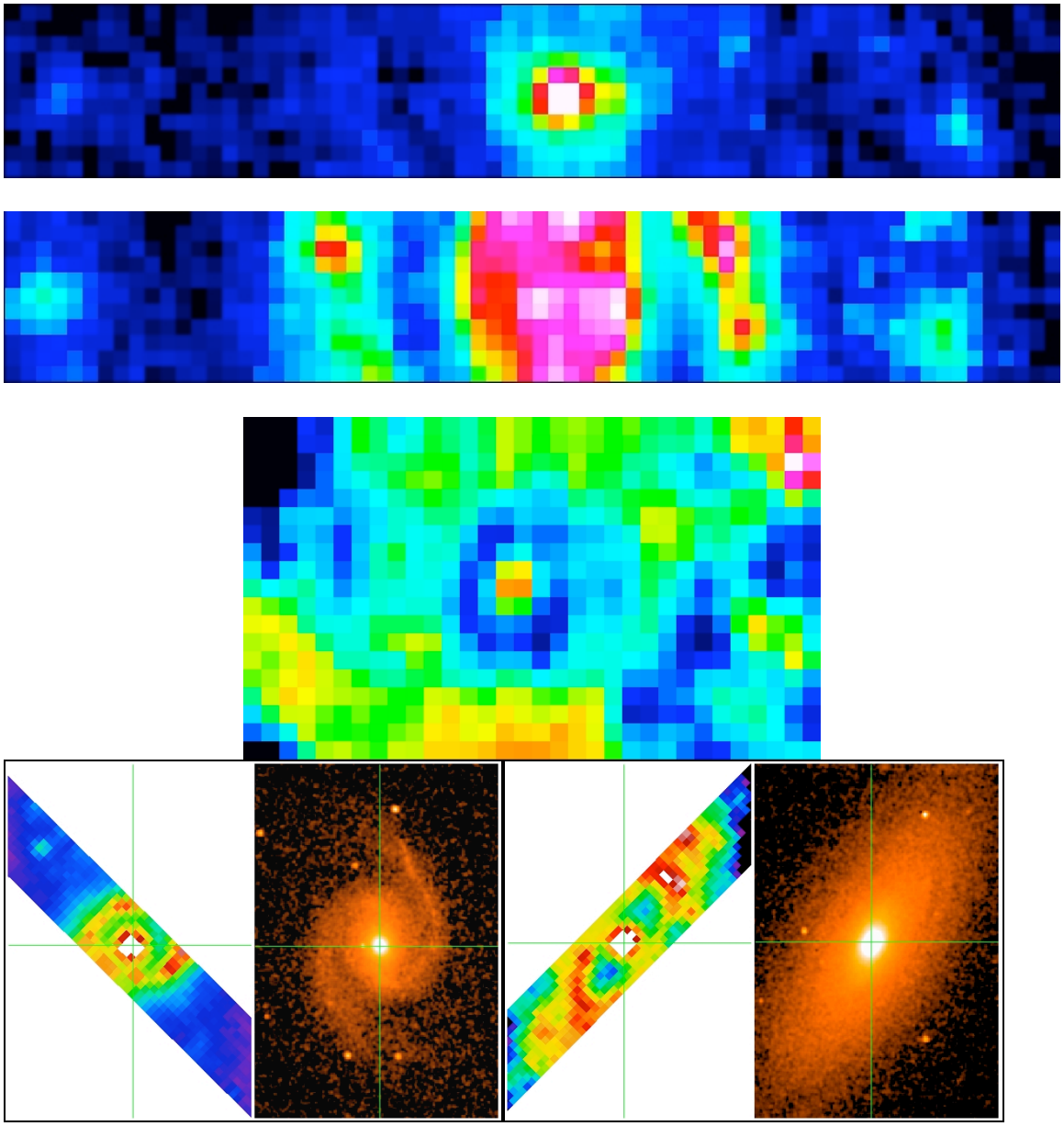

Figure 2. Top 3 panels are examples of DR4 products for NGC 5194. Top panel is the central portion of the continuum-subtracted [NeIII] emission. It is highly centrally concentrated compared to the continuum-subtracted [SiII] emission, shown in the second panel; it shows bright emission in the nucleus and the spiral arms. The third panel shows the integrated PAH emission at 8μm. The fourth and fifth panels show a side-by-side comparison of a 2MASS K-band image and a LL1 map for NGC 1566 and NGC 2841 respectively. The IRS maps have very good astrometry, typically within 1" of the 2MASS coordinates, as indicated by the cross hairs in the last two panels.

The cubes can be viewed and manipulated using the CUBISM software. CUBISM is being developed by the SINGS team and will be released by the SSC shortly. Until then, these data are in the standard fits format and can be examined using any number of available software packages. We have tested the ease of manipulating the cube with the DS9, and KARMA[1] software packages and found it to be compatible with these standard packages for spectral cube analysis. The cubes were readable in MIRIAD[2] but some of the data were masked incorrectly by the program.

6.3 Data Processing & Mapping

S13 processed BCD data were used for this delivery. Below the processing and mapping for the low and high resolution products is discussed separately.

Low-Resolution Products

The low resolution spectral mapping data were assembled into three-dimensional spectral cubes using CUBISM, a tool specifically designed for this purpose (see Kennicutt et al, 2003, Sect. 6.2, and Smith et al. 2006, for more information). Bad pixels are flagged and removed in situ in the redundantly sampled map (typically 10-50 per frame). Background subtraction and flux calibration (described in more detail below) are performed on each cube.

Maps of the nuclear regions are made by averaging the cube along the wavelength dimension over the extraction regions noted above. Line maps are made by continuum-subtracting and integrating the cube over a suitably red shifted wavelength range for the line or feature. The continuum is estimated using a weighted average of nearby continuum values, with weight that varies inversely with the wavelength offset.

A matched rectangular region of 30″×52″ was used to extract the low-resolution spectra for the nuclear regions. (An exception is for NGC7331, our validation galaxy, for which a smaller SL map was obtained, yielding a smaller extraction regions of 15″×52″). The extra nuclear regions are half as wide as the nuclear regions and are extracted from a rectangular region of 15″× 52″. Non-calibrated data at the ends of orders are trimmed in the final spectrum.

[1] See http://www.atnf.csiro.au/computing/software/karma/
[2] See http://bima.astro.umd.edu/miriad/

High-Resolution Products

High resolution maps were also created with CUBISM. In the LH module, the noise is dominated by time varying warm pixels which respond to light, but vary on timescales of days to weeks. This problem is also present in the LL module but is mitigated by background subtraction using the outrigger BCDs (see more below). The SH and SL modules are much less affected by these warm pixels. See the SSC page at http://ssc.spitzer.caltech.edu/irs/roguepixels/ for a more detailed discussion of the behavior and corrections for these pixels. In all cases, the bad pixels were flagged and rejected from the cube building process. In addition, noisy areas at the red and blue ends of each spectral order have been trimmed to create the final, full SH or LH spectral cube, from which fully stitched spectra are extracted. The full low- and high-resolution apertures are not the same size, and their relative orientation depends on the exact dates of the observations because the IRS slits are not parallel in the Spitzer focal plane, and the pixel scale and spatial resolution vary with wavelength. A matched aperture for the full size of the 3×5 SH map, roughly 23″×15″, was used for both high-resolution extractions for nuclear and extra-nuclear regions.

Sky or Background (and Foreground) Subtraction

The sky emission is estimated or taken directly from the maps, and subtracted from all low-resolution maps and spectra. No sky emission was removed from the high-resolution spectra; estimating equivalent widths or other continuum-sensitive measures in high-resolution spectra will require the use of an estimated background spectrum. This may become significant for point sources (either nuclear or extranuclear) with continuum flux densities of 20—30 mJy, or less, or extended sources with a integrated flux of 20—30 mJy over the SL map area. A model of the background at any date and position can be obtained from within SPOT. The background / foreground emission subtraction adopted in this delivery for the low resolution data is described below.

LL: The LL maps, assembled from long radial strips that extend 10' or more across the galaxy, contain a robust measure of the nearby zodiacal and cirrus "background" (which actually is mostly foreground emission). Typically 10-30 spectral frames were averaged together with min/max trimming for subtraction in the 2D spectral image. This process not only removes the background, but also restores many of the time-varying bad pixels to the proper scale.

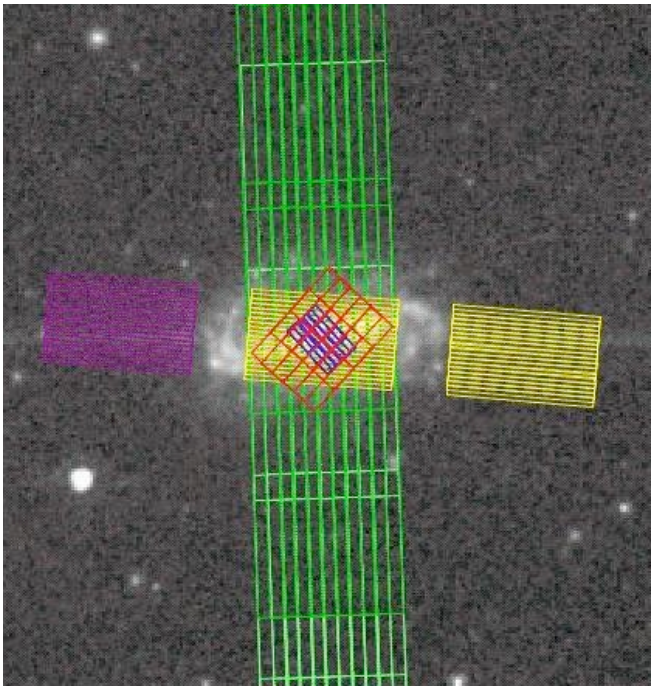

Figure 3: An overlay of the IRS observations on NGC 3049. Notice how the "outrigger" SL2 and SL1 observations serve as a short-low background for this small galaxy. The LL background is determined from the LL BCDs at the ends of the radial strip.

SL: Unlike the LL maps, the SL maps are much smaller, and the background cannot always be measured using the outermost portions of the maps. However, for small galaxies, the areas mapped by the outrigger order may be used for background subtraction. An example where an outrigger map may be used for sky estimation is NGC3049, as shown in Figure 3. This method of using SL outrigger data for sky subtraction was possible for 30 of the 65 galaxies (see Table 2). For another 15 galaxies dedicated off-galaxy sky observations were obtained (labeled "Dedicated" in Table 2).

For galaxies without outrigger or dedicated background spectra, the Spitzer archive was searched for low resolution observations of blank sky within three days of the SINGS observations at approximately the same ecliptic latitude (within 20 degrees). The flux of the background observation(s) was then scaled by linearly combining the background BCDs until the flux in the peak up array of the composite background matched the flux in the galaxy observations. This method produces a SL spectrum which approximates the sky emission for that particular location and time.

For the SL backgrounds for extra-nuclear regions, we used outrigger backgrounds for 33 regions, dedicated off-sky observations for 13, and archival backgrounds for 4 regions. These are listed in Table 3.

Flux Calibration

The flux calibration in the SSC pipeline is optimized for point sources. For these, the extraction aperture is a wavelength-matched expanding aperture chosen to minimize jumps between orders and modules induced by varying fractions of the point spread function. The extracted spectra are trimmed at the ends of orders and fit to a stellar models using a low-order polynomial. For extended sources, however, an expanding aperture is inappropriate since the emission fills the slit[3]. Moreover, the implicit correction for out-of-slit light losses as a function of wavelength, that are applied as a part of the calibration for a point source, need to be *removed* for an extended source. The former correction is referred to as an aperture loss correction function (ALCF) and the latter is referred to as a slit loss correction function (SLCF). We employ an ALCF by deriving a new flux calibration for well-modeled standard stars using a large 28-pixel (non-expanding) extraction aperture. The SLCF for all modules is estimated using a theoretical model of the slit width and instrumental PSF derived from STinyTim. These functions are available with the latest SPICE release from the SSC.

The SLCF is an exact correction only for perfectly uniform (spatially and spectrally) extended sources. Though SINGS sources span a full range of structures, the same uniform slit loss correction is applied to all sources. To estimate the unknown effective pixel solid angles (which relate to the integral over the beam profile of the slit), matched photometry using SINGS MIPS and IRAC maps was employed. We compared the imaging and spectral photometry at 5.7μm (SL2 vs. IRAC3), 8μm (SL1+SL2 vs. IRAC4), and 24μm (LL1 vs. MIPS24). For a limited number of galaxies we also compared the spectral and imaging photometry at 7μm (SL1+SL2 vs. ISOCAM LW2), 15μm (SL1+LL2 vs. ISOCAM LW3) , 16μm (SL1+LL2 vs. IRS Peak-up Blue).
The imaging filter transmission curves were applied to the extracted IRS spectra and the simulated broad band fluxes were compared to the observed fluxes from the IRAC and MIPS images over the same region in all the galaxies; the results of these comparisons were used to derive the effective cube pixel solid angle. The IRAC fluxes, especially in channels 3 and 4 are uncertain for extended sources, but we have used the most recent measurements of the extended source corrections to scale the SL data to match the IRAC photometry. For LL, the photometric comparison with MIPS yields a good match between the pixel solid angle and the empirically measured slit width. The comparison at 15 and 16μm yielded mixed results. Whereas the IRS spectral photometry is in good agreement with the ISOCAM LW3 data, the Peak-Up data give 20-30% higher fluxes. However only nine SINGS galaxies have been mapped with the Blue Peak-Up array. The discrepancy may be in the extended source calibration for the Peak Up array or with the Slit Loss Correction Factor – the latter is uncertain because our sources are extended with unknown a priori spatial and spectral structure. We are investigating these issues further.

[3] See http://ssc.spitzer.caltech.edu/ost/workshop/2005data2/talks/ksheth.pdf

Since we are not able to remove the background from the high-resolution spectra, they have in general a much higher continuum fluxes than the corresponding low-resolution spectra extracted nearby. In addition, we have compared emission line fluxes between the high and low resolution data for three spectral lines ([SIII] at 18.7μm, [SiII] at 34.8μm, [SIII] at 33.4μm) that are in common between high and low resolution modules. We find that on average the [SIII] 18.7 mm line flux is 14% lower in SH than in LL2. For LH, the [SiII] and [SIII] line fluxes are on average 18% lower in SH than LL1. We have corrected the high resolution data to make the line fluxes consistent between the high and low resolution modules. However there is a broad dispersion in the measured fluxes from galaxy to galaxy. Users are reminded that accurate estimates of the equivalent width of spectral features, particularly in regions of low flux, will require a careful background subtraction, which is not performed for these data products.

Effective Integration Times
All spectra delivered are the composite of multiple exposures. For the high resolution data, the effective exposure time per pixel was 4 minutes per pixel. For the low resolution spectra, the integration times were 28s and 60s per pixel for SL and LL respectively. The high resolution data for the extra-nuclear regions was the same but we integrated four times longer in SL.

For a given peak source flux, the signal-to-noise in the resulting spectra depends critically on the spatial distribution of the source. For galaxies with significant extended emission in the extraction regions (e.g. NGC5194), the relative S/N achieved is much higher than for galaxies whose mid-infrared flux is concentrated in the nucleus (e.g. NGC5408). In many cases, higher S/N spectra could be achieved by extracting over smaller regions. However, for consistency among our data products all regions were chosen to be the same size.

6.4 An Estimate of the Uncertainties

Starting with version S12, the SSC pipeline delivers uncertainties in the measurement of the spectra. The uncertainties consist of ramp slope estimation uncertainties that are then propagated during the spectral extractions from individual BCDs. These uncertainties are typically 0.1% at 5 Jy; 0.5--1% at 500 mJy; and 10% at 20 mJy (at low resolution). At high resolution, they are about 1% at 10 Jy. These uncertainties have been incorporated into CUBISM and propagated through the cube building process. Note that the estimates of the uncertainty do not include uncertainties from other sources such as flat-fielding and flux-calibration. As we note below, systematic uncertainties are on the order of 15-20% but the magnitude of the systematic uncertainty can vary as function of wavelength, module and order.

Details of the estimation of uncertainties are described in a presentation at this URL: http://ssc.spitzer.caltech.edu/ost/workshop/2005data2/talks/pappleton.pdf.

6.5 Data Artifacts and Known Problems

Spectral Mismatch and Astrometric Uncertainty
The 4 segments of the low-resolution spectra (SL2, SL1, LL2, LL1, in order of increasing wavelength) are derived from separate spectral cubes with individual astrometric solutions. Astrometric errors typically of order 1.5" can contribute to a mismatch between SL and LL, and, to a lesser degree, to mismatch between orders in the same spectral module (SL1 and SL2, LL1 and LL2). Also contributing to the mismatch is the unknown aperture correction that is made by applying the SLCF which assumes a smooth source brightness distribution.

In many cases users will notice a jump between the SH and LH spectra. The lack of smooth stitching may be because no backgrounds have been subtracted from these data. Another possibility is the small apertures over which the data have been extracted. Since we match the extraction apertures to the SH map, that region involves extraction from a sub-pixel scale from the LH maps. It is also possible that the discrepancy is due to the unknown slit loss correction function, which depends on the source brightness distribution.

Extended Source Flux Calibration
All the spectra have been treated with an aperture loss correction factor, and an approximate slit loss correction factor; the residual systematic uncertainty in these spectra is 15%. Note that the high resolution data do not need an extraction aperture correction because the point source calibration at the SSC is derived by integrating over the full slit. There is uncertainty in the exact correction for extended sources. We mitigate this problem somewhat by scaling the spectra to match the broadband photometric point from MIPS and IRAC but the correction is only approximate because the source brightness distribution is not known a priori. Users are encouraged to keep in mind these corrections especially when estimating line flux ratios, especially for lines in different modules. Users are also reminded that the SH and LH data do not have a background subtracted from them although we have attempted to match the spectra to make line fluxes consistent between the high and low resolution spectra.

Residual Time-Varying Pixels
Responsive, yet time-varying warm pixels are present in all IRS arrays, but they are most problematic for Long-high and Long-low - the two Si:Sb arrays. In particular, Long-High spectra are most affected, since there are many more of these time-varying pixels, and the echelle orders cover a large fraction of the array. For further details about this effect see the discussion on this webpage: http://ssc.spitzer.caltech.edu/irs/roguepixels/. These pixels appear as "spikes" in the final, extracted one-dimensional spectra. While subtraction of campaign-based darks reduces the effect to some degree, much of the SINGS data were taken early in the mission before the problem was fully diagnosed, and before the frequency of dark measurements was increased. We have made a careful attempt to remove residual warm pixels from the two-dimensional BCDs before spectral

extraction, but observers are strongly encouraged to inspect the BCDs if spurious features (sharper than a single resolution element) are present in their spectra. The bulk of the bad pixels for data newly included in the fourth release were identified by automatic detection in the multiple sampling of a given spectrum pixel in the final cube.

Wavelength Calibration Errors
At present the average wavelength uncertainties are less than 0.07μm in the low resolution data, and less than 0.01μm in the high resolution data[4]. Minor errors in some of the high resolution orders noted in the previous documentation have been mitigated with the S13 pipeline data.

Use of the Emission Line Maps
The emission line maps are most useful for assessing the spatial distribution of the line of interest. Accurate line fluxes should be obtained by measuring the line(s) from extracted 1D spectra of the region(s) of interest. Significant uncertainties of order 30% (for a signal to noise ratio greater than 10, and substantially higher for lower signal to noise ratios) are expected for line intensities measured directly from the 2D maps; Users are strongly encouraged to measure line fluxes from the three-dimensional cubes instead of the 2D maps.

6.6 Notes on Individual Galaxies

DDO 154: No IRS data. This galaxy is too faint for IRS observations

Holmberg I: No IRS data. This galaxy is too faint for IRS observations

HolmbergII: No SL, SH or LH data. For the Long-Low spectrum, a square extraction aperture has been employed. The infrared emission peaks 40" from the center of the LL strip.

IC 2574: No IRS data for optical center which is too faint for IRS observations. However we will provide maps for a bright off-center extranuclear region in DR5.

M81 Dwarf A: No IRS data. This galaxy is too faint for IRS observations

M81 Dwarf B: No IRS data. This galaxy is too faint for IRS observations

Tol89: Brightest infrared source is located at the edge of the IRS maps, and is only barely visible in the LL, SL, and LH strips.

NGC0024: problems are present with this galaxy as SL and LL do not match. Neither the dedicated background nor an outrigger background appear to improve the matching. A number of residual glitches are present in the final spectrum.

[4] See the presentation by D. Shupe for the Spitzer Data Analysis workshop at this URL: http://ssc.spitzer.caltech.edu/ost/workshops/2005data/talks/shupe1.pdf

NGC 3034 – No SL, SH or LH nuclear data. The LL strip is perpendcular to the major axis and offset from the center, by design, to avoid a conflict with GTO observations.

NGC 3184 – There is an obvious problem with the SL spectrum of NGC 3184 bluewards of about 9 microns. The SL1 and SL2 orders have a sharp discontinuity at 7.5 microns, with both orders rising steeply to the blue. This problem appears to be partially reduced when extractions are performed over a small aperture centered on the bright nucleus. We suspect that the problem has its origin in the background subtraction, which in this case was archival (see Table 2). Readers are cautioned against using the delivered SL data below 9 microns, while the issue is being investigated.

NGC 5408: The infrared emission peaks 20" from the center of the IRS strips. The peak is absent from the SH and SL strips, and only a portion of it is present in the LH strip. A source external to NGC5408 appears in one of the SL outrigger fields.

NGC 5474: No SL, LL data.

NGC 6822 – No SL, SH or LH nuclear data

NGC 6946_extranuc_03, NGC 6946_extranuc_04, NGC 5194_extranuc_00, and NGC 5194_extranuc_05 - are all contaminated by bright sources that are in their galactic disks but appear in the peak-up arrays. As a result, the SL1 and SL2 stitching is not optimal in the extracted spectra.

Table 2

#	Galaxy	Background
1	DDO 053	Outrigger
2	DDO 165	Outrigger
3	Ho II	No SL data
4	HoIX	Outrigger
5	IC 4710	Outrigger
6	Mrk 33	Outrigger
7	NGC 0024†	Dedicated
8	NGC 0337	Outrigger
9	NGC 0584	Outrigger
10	NGC 0628	Dedicated
11	NGC 0855†	Outrigger
12	NGC 0925†	No SL data
13	NGC 1097	Archival
14	NGC 1266	Dedicated
15	NGC 1291†	Dedicated
16	NGC 1316†	Dedicated
17	NGC 1377	Outrigger
18	NGC 1404	Outrigger
19	NGC 1482†	Outrigger
20	NGC 1512†	Dedicated
21	NGC 1566	Dedicated
22	NGC 1705	Outrigger
23	NGC 2798	Outrigger
24	NGC 2841	Model 1-D
25	NGC 2915	Outrigger
26	NGC 2976	Archival
27	NGC 3034†	No SL data
28	NGC 3049	Outrigger
29	NGC 3184	Archival
30	NGC 3190	Outrigger
31	NGC 3198	Archival
32	NGC 3265	Outrigger
33	NGC 3351	Dedicated
34	NGC 3521	Model 1-D
35	NGC 3621	Archival
36	NGC 3627	Archival
37	NGC 3773	Outrigger
38	NGC 3938	Archival
39	NGC 4125	Outrigger
40	NGC 4236†	Dedicated
41	NGC 4254	Archival
42	NGC 4321	Archival
43	NGC 4536	Outrigger
44	NGC 4552	Outrigger
45	NGC 4569	Archival
46	NGC 4579	Dedicated
47	NGC 4594†	Dedicated
48	NGC 4625†	Outrigger
49	NGC 4631†	Outrigger
50	NGC 4725	Archival
51	NGC 4736	Model 1-D
52	NGC 4826	Outrigger
53	NGC 5055†	Dedicated
54	NGC 5194	Archival
55	NGC 5195†	Dedicated
56	NGC 5408	Outrigger
57	NGC 5474†	No SL data
58	NGC 5713	Outrigger
59	NGC 5866	Outrigger
60	NGC 6822	No SL data
61	NGC 6946	Dedicated
62	NGC 7331	Dedicated
63	NGC 7552†	Outrigger
64	NGC 7793†	Dedicated
65	Tol 89	Outrigger

Galaxies with IRS data in this delivery of SINGS products. † indicates galaxies for which the three dimensional cubes will be delivered next time in the fifth and last delivery. Different types of backgrounds as indicated in the third column for each set. As discussed in the text, Dedicated means sky observations obtained immediately following the mapping, Outrigger indicates sky background estimated from outer parts of a SL or LL map, Archival means that the background was estimated from nearest in time archive spectra, Model-1D indicates an approximation to the background based on models and the observed 24μm flux.

Table 3

#	Extranuclear Region	Background
1	ngc5194_extranuc_00	Outrigger
2	ngc5194_extranuc_01	Outrigger
3	ngc5194_extranuc_02	Outrigger
4	ngc5194_extranuc_03	Outrigger
5	ngc5194_extranuc_04	Outrigger
6	ngc5194_extranuc_05	Outrigger
7	ngc3031_extranuc_00	Outrigger
8	ngc3031_extranuc_01	Outrigger
9	ngc3031_extranuc_02	Outrigger
10	ngc3031_extranuc_03	Outrigger
11	ngc3031_extranuc_04	Outrigger
12	ngc3031_extranuc_05	Outrigger
13	ngc3031_extranuc_06	Outrigger
14	ngc6946_extranuc_00	Outrigger
15	ngc6946_extranuc_01	Outrigger
16	ngc6946_extranuc_02	Outrigger
17	ngc6946_extranuc_03	Outrigger
18	ngc6946_extranuc_04	Outrigger
19	ngc0628_extranuc_00	Outrigger
20	ngc0628_extranuc_01	Outrigger
21	ngc0628_extranuc_02	Outrigger
22	ngc0628_extranuc_03	Outrigger
23	hoii_extranuc_00	Outrigger
24	hoii_extranuc_01	Outrigger
25	hoii_extranuc_02	Outrigger
26	hoii_extranuc_03	Outrigger
27	ngc4736_extranuc_00	Outrigger
28	ngc4736_extranuc_01	Outrigger
29	ngc4736_extranuc_02	Outrigger
30	ngc6822_extranuc_00	Outrigger
31	ngc6822_extranuc_01	Outrigger
32	ngc6822_extranuc_02	Outrigger
33	ngc6822_extranuc_03	Outrigger
34	ngc6946_extranuc_05	Archival
35	ngc6946_extranuc_06	Archival
36	ngc6946_extranuc_07	Archival
37	ngc6946_extranuc_08	Archival
38	ngc5194_extranuc_10	Dedicated
39	ngc6822_extranuc_00	Dedicated
40	ngc6822_extranuc_01	Dedicated
41	ngc6822_extranuc_02	Dedicated
42	hoii_extranuc_04	Dedicated
43	ngc3521_extranuc_00	Dedicated
44	ngc3521_extranuc_01	Dedicated
45	ngc3521_extranuc_02	Dedicated
46	ngc3521_extranuc_03	Dedicated
47	ngc7793_extranuc_00	Dedicated
48	ngc7793_extranuc_01	Dedicated
49	ngc7793_extranuc_02	Dedicated
50	ngc7793_extranuc_03	Dedicated

For the extra-nuclear regions (1—25) full three-dimensional cubes are delivered. The right column in the Table indicates the type of background used in each case as discussed in the text.

7. Ancillary Data

7.1 Optical Imaging

Observations

Optical images for the galaxies in the SINGS sample were obtained at NOAO, as part of the Legacy Project, over the course of about 3 years (2001-2003). Observations were carried out at both the KPNO 2.1-m and the CTIO 1.5-m telescopes, using standard broad band B, V, R, and I filters, and a set of narrow-band filters in correspondence of the redshifted Hα line emission (0.6563 μm). The characteristics of the narrow-band filters (from the NOAO Web pages) are as follows:

Filter Name	Central Wavelength	FWHM	Peak Transmission
KP1468 (KPNO)	6567 A	84 A	72 %
KP1563 (KPNO)	6573 A	67 A	83 %
KP1390 (KPNO)	6587 A	72 A	67 %
KP1564 (KPNO)	6618 A	74 A	79 %
CT6568 (CTIO)	6568 A	19 A	70 %
CT6586 (CTIO)	6583 A	20 A	71 %
CT6602 (CTIO)	6596 A	18 A	70 %
CT6618 (CTIO)	6610 A	18 A	72 %

The 2Kx2K CCDs used for the observations have field-of-view (FOV) of 10' and 14.5', and pixel scale 0."305 and 0."433, at the KPNO-2.1-m and at the CTIO-1.5-m telescopes, respectively. Galaxies more extended than the CCD FOVs were imaged at multiple, overlapping pointings.

Exposure times ranged from 240 seconds to 1400 seconds (typically split into 2 separate exposures for cosmic ray removal.), in order to reach uniform depth of about 25 mag/arcsec^2 with signal-to-noise ratio of ~10 in the broad-band filters. Exposure times in the narrow-band filters were typically 1800 seconds, split into two separate exposures. In a minority of cases, a single narrow-band exposure was available.

Data Processing

Data reduction consisted of bias subtraction (using also the overscan region in the case of the KPNO images), flat-fielding (with both dome- and twilight-flats), single-image cosmic ray removal, and combination of pairs (or multiple) images at the same pointing/filter.

The southern 3' of the CCD FOV at the KPNO-2.1-m suffers from pronounced **vignetting**, whose intensity is pointing-dependent. We developed a routine to remove as much as possible of the vignetting effect from each frame. The corrected frames were then used to create the final mosaics. See the section on `Known Problems' below for a quantification of the effectiveness of the vignetting-removal routine.

Astrometric solutions were derived for all optical images/mosaics, and the appropriate WCS keywords (FITS standard) stored in the image headers. All delivered optical images/mosaics have been rotated to the standard NE orientation.

Photometric and spectrophotometric standard stars were observed during each observing run to flux calibrate the images/mosaics. The spectrophotometric stars (e.g., Feige 34, HZ44) were used to obtain flux calibrations for the narrow-band filters. Effects of vignetting were negligible on the standard star frames, as the stars were usually centered on the CCD FOV, thus avoiding the vignetted edge.

Data Characteristics

All delivered optical images are in units of counts-per-seconds (CPS, stored in the UNITS keyword). The flux conversion keyword is PHOTFLAM, with units of Jy*sec/DN/pixel, as given by the keyword ZUNITS. Zeropoints are stored in the keyword ZPOINT (in Jy). For the narrow-band images, the keyword FILTER records the name of the filter utilized for the observations (e.g., KP1563, CT6602, etc.).

The images are **not** background-subtracted. The narrow-band images (*_HA.fits) generally contain emission from Hα, as well as the [NII]($\lambda\lambda$ 6548,6584), along with underlying stellar continuum. **Stellar continuum-subtracted narrow-band** images are also provided as *_HA_SUB.fits for most of the galaxies (this is the only optical image delivered for NGC5408, together with its rescaled continuum, and for NGC5055). Users can also construct their own pure emission-line images by scaling and subtracting the R-band images from the narrow-band images.

Most images have photometric accuracy within 5% (broad band) or 10% (narrow band). Care was taken to re-observe in photometric conditions any galaxy that had been previously acquired in non-photometric conditions. When this could not be accomplished (or there were larger-than-usual uncertainties in the standard stars calibrations) a COMMENT keyword was added to the image header. When more than one comment line is present, suffixes (COMMENT1, COMMENT2, etc.) are used.

In addition to astrometric and photometric keywords, the image headers contain other useful keywords detailing the observations (e.g., telescope, camera, filters, exposure times, etc.).

Conversion from count-rates to fluxes/magnitudes

Conversions from count-rates (CPS) to standard (Vega) magnitude scales for the optical images are accomplished with the following formula:

$$m = -2.5 * [\log(CPS*PHOTFLAM) - \log(ZPOINT)]$$

To convert continuum-subtracted narrow-band images from CPS to more familiar units for emission lines, e.g., erg s^{-1} cm^{-2}:

$$F(\text{erg s}^{-1}\ \text{cm}^{-2}) = 3\text{E-}5 * \text{CPS}*\text{PHOTFLAM}*\text{FWHM} / \text{CW}^2$$

where FWHM and CW are the full-width half maximum and the central wavelength of the narrow-band filter, respectively. If the emission line(s) are shifted from the center of the filter's bandwidth, additional corrections for the filter's transmission curve need to be included in the above formula.

Known Problems

Comparison of the fluxes of stars in common between adjacent, overlapping pointings indicate that the vignetting-correction routine usually brings stellar fluxes into agreement within 2%-3%, but deviations as large as 5%-10% are not uncommon. Such residuals are often visible as `seams' at the overlapping points of adjacent frames.

Notes on individual galaxies:

Short Exposures: short (60 s) exposures are delivered for a small set of the galaxies, for which saturation of the central region could constitute a concern. The galaxies are: HoII (R), IC2574 (R), NGC3031 (R), NGC5194 (V,R,I). The images are called: XXXX_#_short_dr4.fits (where XXXX=galaxy name and #=filter's name).

NGC0855 and NGC4569: no optical images available for these galaxies.

DDO053, HoI, HoIX, M81DwA, M81DwB, NGC2915, NGC4625, NGC4736, NGC5033: no Hα images available for these galaxies.

NGC2798: residual fixed pattern noise present in all images. This is present in both unreduced and reduced images, and in the dark and bias frames as well.

NGC2915: no B and Hα images available.

NGC2976 and NGC3049: residual fixed pattern noise is present in the narrow-band images.

NGC3031: only R and Hα images are available.

NGC3198: Marginal seeing conditions (broad PSF).

NGC3351 and NGC3521: BVI images for these galaxies are from the KPNO-4m plus MOSAIC Imager. The pixel scale is 0.27 arcsec/pixel. For NGC3351, no continuum-subtracted narrow-band image is delivered. The V-band image of NGC3521 shows a high-noise banding across the target.

NGC3621: images are from the CTIO-4m plus MOSAIC II. The pixel scale is 0.27 arcsec/pixel.

NGC3627: KP1564 was used as Hα filter; in the filter's bandpass, Hα is at ~30% level in the transmission curve, while [NII](6584 A) is at 70%.

NGC3773: Fixed pattern noise is present in the I and narrow band images.

NGC4559: The Hα image for this galaxy is split into two frames (NW and SE); the two images could not be combined together, as the atmospheric conditions (seeing) were very different between the two observations.

NGC4725: Only the NE frame is available for the B band.

NGC4736: KP1564 was used as Hα filter; however, its bandpass does not contain the Hα emission from the galaxy, and only the [NII](6584 A) emission was observed. The narrow band image for NGC4736 is delivered as ngc4736_NII.fits and ngc4736_NII_SUB.fits.

NGC4826: Optical images are from the SONG collaboration. The pixel scale is approximately 0.777 arcsec/pixel. The Hα image is already continuum-subtracted (information stored in the image header as COMMENT* keyword). A few bad columns (190-195) have been interpolated across, for the B, V, R, and I images. No calibration scales could be obtained for the R and I bands. No zeropoints available.

NGC5055: The continuum-subtracted Hα image is from the SONG collaboration. This is the only image available for this galaxy.

NGC5194: In addition to the nominal mosaics, a set of short-exposure mosaics are delivered for the V, R, and I bands, to aid treatment of the saturated nucleus of the galaxy. Residual vignetting is particularly noticeable in the R and I-band images of this galaxy, along the EW seam between the two overlapping pointings, and especially at the western side of the seam. In this latter region, the effect of the residual vignetting translates into an 8% variation in the surface brightness of the galaxy across the seam, at a position located 174 arcsec west of the nucleus. The surface brightness at this location is about 360 times fainter than the nuclear one. The effects of residual vignetting become worse westward of this point, and quickly decrease in magnitude eastward of this point.

NGC5408: only the continuum-subtracted Hα and adjacent continuum images are available for this galaxy.

7.2 Optical Spectroscopy

Observations

Optical spectra for the SINGS galaxies in the wavelength range 0.36-0.70 μm, with resolution ~8 Angstrom, were obtained at the 2.3-meter Bok telescope with the B&C spectrograph, and at the 1.5-meter CTIO telescope with CSPEC.

Three types of long-slit spectra were obtained:

- Nuclear spectra: a 2".5 wide aperture (3" at CTIO) was pointed at the brightest central spot of the galaxy;
- 20" drift scans: the slit was drifted for 20" around the central region, while exposing;
- 55" drift scans: similar to the 20" drift scans, with a scan length of 55".

The data were taken during clear, photometric or semi-photometric conditions. A minimum of two sequential exposures were taken to facilitate cosmic-ray rejection. The total exposure times ranged from 600 seconds for the nuclear pointings to 900-2400 seconds for the 20" and 55" drift-scanned spectra. In the drift-scanned spectra the *effective* exposure time, t_effective, spent on a single spatial position of the galaxy is given by:

t_effective = t_exposure * (Aperture / Delta),

where t_exposure is the actual exposure time, Delta is the length of the scan in arcseconds (here, 20" or 55"), and Aperture is the slit width in arcseconds (here, 2.5" or 3"; see Kennicutt 1992, ApJS, 79, 255, and Moustakas & Kennicutt 2005, ApJS, submitted, for details).

Data Processing

The two-dimensional spectra were reduced with iSPEC2d, a customized longslit data reduction package developed in IDL by John Moustakas (UofA). The data were overscan- and bias-subtracted, trimmed, flat-fielded, and corrected for a low-order illumination pattern. The two-dimensional sky spectrum was subtracted from each image before rebinning using the technique described in Kelson (2003, PASP, 115, 688). Sequential exposures were combined to reject cosmic rays; residual cosmic rays and hot pixels were flagged using LA_COSMIC (van Dokkum 2001, PASP, 113, 1420) and interpolated. The data were then wavelength- and flux-calibrated. Although standard stars were taken through good sky and seeing conditions, absolute spectrophotometric accuracy is not guaranteed, especially for the 2.5 arcsec nuclear spectra where slit losses from seeing may be significant. The relative spectrophotometric accuracy ranges from 1-4% based on the relative scatter in the derived sensitivity function. Two-dimensional error maps are generated using the known noise properties of the CCD and assuming Poisson statistics. These error maps are processed identically to the data.

One-dimensional data, error, and sky spectra were extracted in a 2.5" aperture for the nuclear spectra and a 20" aperture for the drift-scanned spectra using a low-order trace. A small wavelength shift was applied to the final wavelength solution by centroiding on the [O I] 5577 night sky line. The spectra have been de-reddened for foreground Galactic extinction assuming the O'Donnell (1994, ApJ, 422, 158) extinction curve and using the Schlegel, Finkbeiner, & Davis (1998, ApJ, 500, 525) reddening maps. The 20” drift-scan spectra accompany the equivalent-size extraction 1D IRS spectra.

Data Characteristics

The data are stored as ASCII files with the following columns:

1 – wavelength	[Angstrom]
2 – sky-subtracted data spectrum	[erg s^{-1} cm^{-2} A^{-1}]
3 - error spectrum	[erg s^{-1} cm^{-2} A^{-1}]
4 - sky spectrum	[erg s^{-1} cm^{-2} A^{-1}]

At the beginning of each file, basic information on the slit center is also reported.

The file names indicate the type of spectrum ("drift" or "nuclear"), the drift scan length, and the extraction aperture in arseconds. For example, in "ngc0337_drift_020_020.txt", the first "020" is the scan-length while the second "020" is the aperture width. In "ngc0337_nuclear_002.5.txt" only one number appears indicating the extraction aperture.

***Notes on individual galaxies**:*

Ngc0337: Ill-defined nucleus, the tracing (placement of the extraction aperture's center) along the wavelength direction was not optimal.

DDO053, HolmbergIX, IC2574, DDO165, NGC2976 and Tol89: only the central 20"x20" drift-scan spectrum is available.

NGC5713: only the nuclear spectrum is available.

DDO154, HombergII, IC4710, NGC5408, NGC6822, and NGC7552: No spectra available for these galaxies.

8. Acknowledgements

The SINGS Team wishes to acknowledge contributions from the following people: John Moustakas (UofA), for obtaining, reducing, and processing the optical spectra; Megan Sosey (STScI), for reducing and processing the optical images; Janice Lee and Sanae Akiyama (UofA), for help in deriving the continuum-subtracted Hα images; Max Mutchler and Helene McLaughlin (STScI), for help processing the IRAC mosaics.
We also wish to thank the MIPS Instrument Team for the use of their pipeline for the reduction and processing of the MIPS mosaics.